

# Supporting Information

**Order in the chaos: The secret of the large negative entropy of  
dissolving 1-alkyl-3-methylimidazolium chloride in  
trihexyltetradecylphosphonium chloride**

Stefan Zahn<sup>a,\*</sup>,<sup>1</sup> and Annegret Stark<sup>b,\*</sup>,<sup>2</sup>

<sup>a</sup>Wilhelm Ostwald Institut für Physikalische und Theoretische Chemie,  
Universität Leipzig, Linnéstr. 2, 04103 Leipzig, Germany

<sup>b</sup>Eduard-Zintl Institut for Inorganic and Physical Chemistry,  
Technical University Darmstadt, Alarich-Weiss-Straße 8, 64287 Darmstadt, Germany

---

<sup>1</sup>email: stefan.zahn@uni-leipzig.de

<sup>2</sup>email: annegret.stark@outlook.de

# 1 Computational Details

## 1.1 Classical Molecular Dynamics Simulations

Large systems and long simulation run times are needed to obtain correct dynamical properties of ionic liquids.<sup>1</sup> Therefore, all NVT simulations consisted of a cubic box enclosing 512 ion pairs and the simulation run time was 50 ns. A time step of 2 fs was selected in the production run and data points were collected for the analyzed trajectories every 10 ps. The box length was determined by NPT simulations of 2 ns run time which were equilibrated at least 2.5 ns. The obtained box length of each NVT simulation can be found in table 1. Temperature was kept constant by a Nosé–Hoover chain thermostat<sup>2–4</sup> in all simulations (T=400 K,  $\tau=200$  fs) and the SHAKE algorithm<sup>5</sup> was employed to constrain all C-H bonds during the simulations. The particle-particle particle-mesh solver<sup>6</sup> was used to calculate Coulomb interaction energies beyond the cutoff which was set to 1000 pm. All employed force field parameters were taken from the OPLS-AA/AMBER all atom force field developed for ionic liquids by Canongia Lopes *et al.*<sup>7–11</sup> LAMMPS<sup>12</sup> was used to carry out all classical molecular dynamics simulations while TRAVIS<sup>13</sup> was employed to analyze the obtained trajectories.<sup>13</sup>

**Table 1:** Simulation box length  $l$  in pm, density  $\rho$  in  $\text{g}/\text{cm}^3$  of the NVT simulations (T = 400 K), and abbreviations for all investigated systems.

systematic abbreviation <sup>14</sup>	abbr.	$l$	$\rho$
[C <sub>2</sub> C <sub>1</sub> im][Cl]	<b>pure-E</b>	4870.0	1.079
[C <sub>6</sub> C <sub>1</sub> im][Cl]	<b>pure-H</b>	5655.2	0.953
[C <sub>6</sub> C <sub>6</sub> C <sub>6</sub> C <sub>14</sub> P][Cl]	<b>pure-P</b>	8261.6	0.783
[C <sub>2</sub> C <sub>1</sub> im] <sub>0.125</sub> [C <sub>6</sub> C <sub>6</sub> C <sub>6</sub> C <sub>14</sub> P] <sub>0.875</sub> [Cl]	<b>mix-E</b>	7976.1	0.792
[C <sub>6</sub> C <sub>1</sub> im] <sub>0.125</sub> [C <sub>6</sub> C <sub>6</sub> C <sub>6</sub> C <sub>14</sub> P] <sub>0.875</sub> [Cl]	<b>mix-H</b>	8023.2	0.790

We have chosen  $[\text{C}_2\text{C}_1\text{im}]\text{Cl}$  instead of  $[\text{C}_1\text{C}_1\text{im}]\text{Cl}$  in our molecular dynamics simulations for following reasons:

1. The negative entropy of dissolving  $[\text{C}_2\text{C}_1\text{im}]\text{Cl}$  in  $[\text{C}_6\text{C}_6\text{C}_6\text{C}_{14}\text{P}]\text{Cl}$  is still large ( $-39.1 \text{ J/K}\cdot\text{mol}$ ).<sup>15</sup> Furthermore, the negative entropy decreases systematically with increasing alkyl chain length at the imidazolium cation. Thus, it can be expected that the structure motif responsible for the large negative entropy of dissolving  $[\text{C}_1\text{C}_1\text{im}]\text{Cl}$  in  $[\text{C}_6\text{C}_6\text{C}_6\text{C}_{14}\text{P}]\text{Cl}$  is still conserved in  $[\text{C}_2\text{C}_1\text{im}]\text{Cl}$ . To prove this, we have simulated a system consisting of 448  $[\text{C}_6\text{C}_6\text{C}_6\text{C}_{14}\text{P}]\text{Cl}$  ion pairs and 64  $[\text{C}_1\text{C}_1\text{im}]\text{Cl}$  ion pairs (**mix-M**) for 5 ns at 400 K. The cubic box length was set to 7967.3 pm and every 10 ps was collected one data point. The spatial distribution around the imidazolium cation of **mix-M** is shown in Fig. 1 of the supporting information. The similarity of the shown spatial distribution for this system to the one of **mix-E** is clearly visible.
2. At 400 K, about 10 mol % of  $[\text{C}_2\text{C}_1\text{im}]\text{Cl}$  are soluble in  $[\text{C}_6\text{C}_6\text{C}_6\text{C}_{14}\text{P}]\text{Cl}$  while only about 2 mol % of  $[\text{C}_1\text{C}_1\text{im}]\text{Cl}$  are soluble in  $[\text{C}_6\text{C}_6\text{C}_6\text{C}_{14}\text{P}]\text{Cl}$ .<sup>15</sup> Thus, the selected composition of 1  $[\text{C}_2\text{C}_1\text{im}]$  : 7  $[\text{C}_6\text{C}_6\text{C}_6\text{C}_{14}\text{P}]$  for the investigated mixture **mix-E** is close to the experimental limit. If  $[\text{C}_1\text{C}_1\text{im}]$  is selected instead, the ratio should be 1  $[\text{C}_1\text{C}_1\text{im}]$  : 49  $[\text{C}_6\text{C}_6\text{C}_6\text{C}_{14}\text{P}]$ . Thus, only about 10 imidazolium cations will be in a simulation box of 500 ion pairs which will result in a poor sampling due to the high viscosity of the phosphonium based ionic liquid and the small number of imidazolium cations.
3. The melting point of  $[\text{C}_1\text{C}_1\text{im}]\text{Cl}$  is above 100 °C. Since we compared properties of the pure compounds to the mixture, all simulations should be carried out at the same temperature. Unfortunately, the solubility of  $[\text{C}_1\text{C}_1\text{im}]\text{Cl}$  in  $[\text{C}_6\text{C}_6\text{C}_6\text{C}_{14}\text{P}]\text{Cl}$  decreases significantly with increasing temperature.<sup>15</sup> Thus, increasing the simulation temperature further does not seem reasonable.
4. It is very well known that the chloride anion resides mainly close to the C2-H2 vector but not in front of the most acidic proton H2 in the force field model of Canongia Lopes *et al.* while it prefers a position in front of the acidic proton H2 in ab initio molecular

dynamics simulations.<sup>16,17</sup> Therefore, a highly symmetric arrangement similar like in **cage-Im** can not be obtained by the employed force field. Nonetheless, a recent study has shown that the force field of Canongia Lopes *et al.* is most reliable for the hydrogen bond structure compared to three other force field models of imidazolium based ionic liquids.<sup>18</sup> Since our study focuses on structure properties, we selected the force field of Canongia Lopes *et al.*

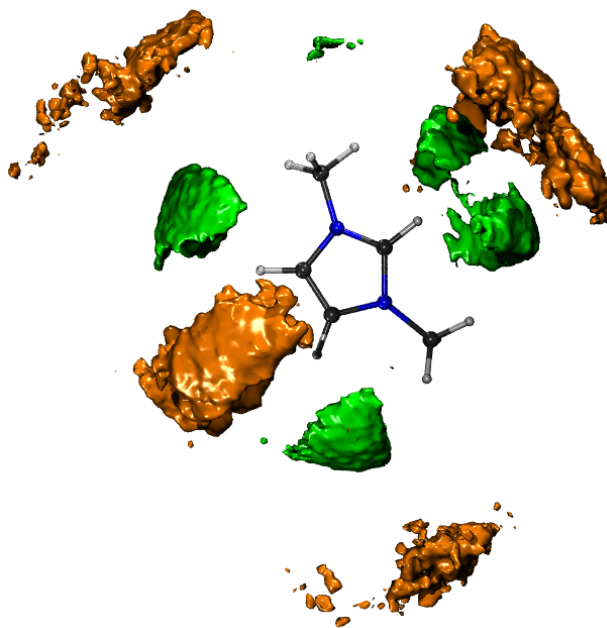


**Figure 1:** Spatial distribution of chloride (*green*) and P (*orange*) around the imidazolium plane of **mix-M**

## 1.2 Static Quantum Chemistry Calculations

The programs provided by the Turbomole-suite<sup>19</sup> were applied for all calculations for which the BLYP-D2<sup>20-22</sup> functional in combination with the 6-31++G\*\* basis set<sup>23,24</sup> and the resolution of identity approximation<sup>25-27</sup> was employed. Several studies have shown that Kohn-Sham density functional theory calculations with an empirical dispersion correction produce reliable results.<sup>28-33</sup> Solvation effects were considered by the COnductor-like Screening MOdel<sup>34</sup> (COSMO) in which the dielectric constant  $\epsilon$  was set to  $\infty$ . Computational stud-

ies pointed to strong charge screening in ionic liquids.<sup>35,36</sup> Therefore, a dielectric constant  $\epsilon = \infty$  was suggested as a more appropriate value than the small measured experimental one to model ionic liquid solvation in computational models.<sup>35</sup>

## 2 Radial Pair Distribution Functions

Radial pair distribution functions (RDF) give the probability to find an atom at a certain distance from another reference atom and, therefore, contain the information of the average nearest neighbor distance and the structuring of the liquid. A value of one represents statistical distribution at the related distance. A comparison of the H2-Cl-RDFs, the H4-Cl-RDFs, the H5-Cl-RDFs, the P-Cl-RDFs and the P-P-RDFs can be seen in Fig. 3 of the supporting information. All atom labels can be found in Fig. 2.

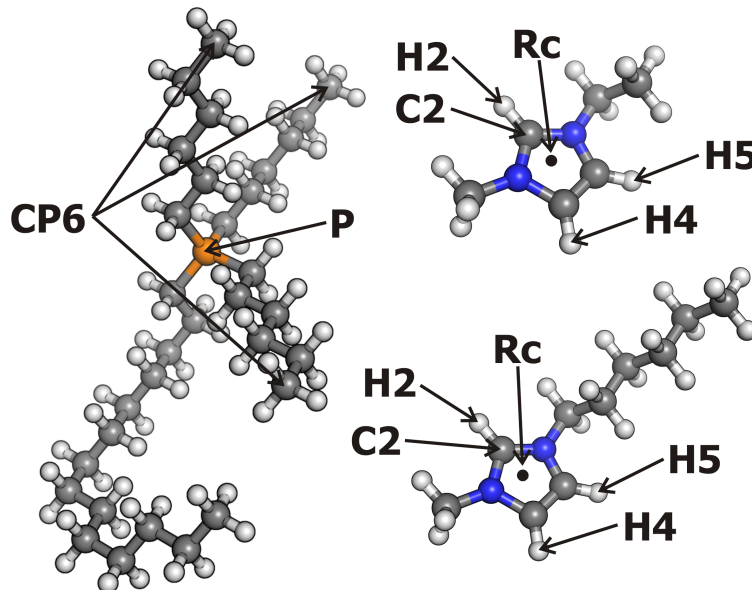


**Figure 2:** Ball-and-stick model of all cations in the investigated systems with atom labels used throughout this work. Rc is the geometric ring center of the imidazolium cation.

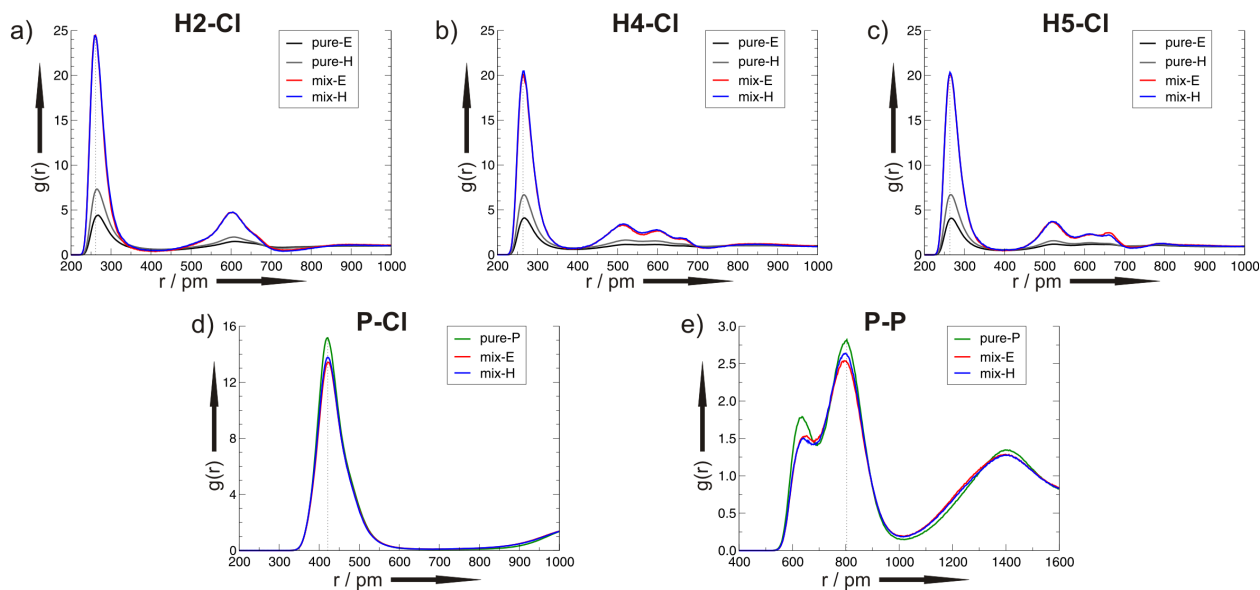


**Figure 3:** Comparison of RDFs of the investigated ionic liquid systems

## References

- [1] Gabl, S.; Schröder, C.; Steinhauser, O. *J. Chem. Phys.* **2012**, *137*, 094501.
- [2] Nosé, S. *J. Chem. Phys.* **1984**, *81*, 511–519.
- [3] Hoover, W. G. *Phys. Rev. A* **1985**, *31*, 1695–1697.
- [4] Martyna, G. J.; Klein, M. L.; Tuckerman, M. *J. Chem. Phys.* **1992**, *97*, 2635–2643.
- [5] Ryckaert, J.-P.; Ciccotti, G.; Berendsen, H. J. C. *J. Comput. Phys.* **1977**, *23*, 327–341.
- [6] Hockney, R. W.; Eastwood, J. W. *Computer Simulation Using Particles*; McGraw-Hill, 1981.
- [7] Cornell, W. D.; Cieplak, P.; Bayly, C. I.; Gould, I. R.; Merz, K. M.; Ferguson, D. M.; Spellmeyer, D. C.; Fox, T.; Caldwell, J. W.; Kollman, P. A. *J. Am. Chem. Soc.* **1995**, *117*, 5179.
- [8] Jorgensen, W. L.; Maxwell, D. S.; Tirado-Rives, J. *J. Am. Chem. Soc.* **1996**, *118*, 1225–11236.

- [9] Canongia Lopes, J. N.; Deschamps, J.; Pádua, A. A. H. *J. Phys. Chem. B* **2004**, *108*, 2038–2047.
- [10] Canongia Lopes, J. N.; Deschamps, J.; Pádua, A. A. H. *J. Phys. Chem. B* **2004**, *108*, 11250–11250.
- [11] Canongia Lopes, J. N.; Pádua, A. A. H. *J. Phys. Chem. B* **2006**, *110*, 19586–19592.
- [12] Plimpton, S. *J. Comp. Phys.* **1995**, *117*, 1–19.
- [13] Brehm, M.; Kirchner, B. *J. Chem. Inf. Model.* **2011**, *51*, 2007–2023.
- [14] Niedermeyer, H.; Hallett, J. P.; Villar-Garcia, I. J.; Hunt, P. A.; Welton, T. *Chem. Soc. Rev.* **2012**, *41*, 7780–7802.
- [15] Arce, A.; Earle, M. J.; Katdare, S. P.; Rodríguez, H.; Seddon, K. R. *Chem. Commun.* **2006**, 2548–2550.
- [16] Del Pópolo, M.; Lynden-Bell, R.; Kohanoff, J. *J. Phys. Chem. B* **2005**, *109*, 5895–5902.
- [17] Bhargava, B.; Balasubramanian, S. *Chem. Phys. Lett.* **2006**, *417*, 486–491.
- [18] Zahn, S.; Cybik, R. *American Journal of Nano Research and Application* **2014**, accepted.
- [19] Ahlrichs, R.; Bär, M.; Häser, M.; Horn, H.; Kölmel, C. *Chem. Phys. Lett.* **1989**, *162*, 165–169.
- [20] Becke, A. D. *Phys. Rev. A* **1988**, *38*, 3098–3100.
- [21] Lee, C.; Yang, W.; Parr, R. G. *Phys. Rev. B* **1988**, *37*, 785–789.
- [22] Grimme, S. *J. Comput. Chem.* **2006**, *27*, 1787–1799.
- [23] Hehre, W. J.; Ditchfield, R.; Pople, J. A. *J. Chem. Phys.* **1972**, *56*, 2257–2261.
- [24] Francl, M. M.; Pietro, W. J.; Hehre, W. J.; Binkley, J. S.; Gordon, M. S.; DeFrees, D. J.; Pople, J. A. *J. Chem. Phys.* **1982**, *77*, 3654–3665.

- [25] Baerends, E. J.; Ellis, D. E.; Ros, P. *Chem. Phys.* **1973**, *2*, 41–51.
- [26] Dunlap, B. I.; Connolly, J. W. D.; Sabin, J. R. *J. Chem. Phys.* **1979**, *71*, 3396–3402.
- [27] Weigend, F. *Phys. Chem. Chem. Phys.* **2006**, *8*, 1057–1065.
- [28] Del Pópolo, M. G.; Pinilla, C.; Ballone, P. *J. Chem. Phys.* **2007**, *126*, 144705.
- [29] Zahn, S.; Kirchner, B. *J. Phys. Chem. A* **2008**, *112*, 8430–8435.
- [30] Izgorodina, E. I.; Bernard, U. L.; MacFarlane, D. R. *J. Phys. Chem. A* **2009**, *113*, 7064–7072.
- [31] Kohanoff, J.; Pinilla, C.; Youngs, T. G. A.; Artacho, E.; Soler, J. M. *J. Chem. Phys.* **2011**, *135*, 154505.
- [32] Grimme, S.; Hujo, W.; Kirchner, B. *Phys. Chem. Chem. Phys.* **2012**, *14*, 4875–4883.
- [33] Zahn, S.; MacFarlane, D. R.; Izgorodina, E. I. *Phys. Chem. Chem. Phys.* **2013**, *15*, 13664–13675.
- [34] Klamt, A.; Schüürmann, G. *J. Chem. Soc., Perkin Trans. 2* **1993**, 799–805.
- [35] Lynden-Bell, R. M. *Phys. Chem. Chem. Phys.* **2010**, *12*, 1733–1740.
- [36] Wendler, K.; Zahn, S.; Dommert, F.; Berger, R.; Holm, C.; Kirchner, B.; Delle Site, L. *J. Chem. Theory Comput.* **2011**, *7*, 3040–3044.